Supporting Information

Carbon-Coated FeCoNi Nanocatalysts for the Electrocatalytic Oxygen Reduction Reaction

Haitao Huang, [a,d] Chengcheng Zhang,[b] Haijin Li,[a,b,c,*] Jianmin Wang,[b] Zhijie Chen,[b] Yitao He,[b] Yongtao Li,[a,b,c,*] Jing Hu, [b] Xiaofang Liu, [b,*] Xiaolong Deng, [a,e] Shaochun Shi [f]

[a] Low-Carbon New Materials Research Center, Low-Carbon Research Institute, Anhui University of Technology, Ma'anshan, 243002, P. R. China

[b] School of Energy and Environment, Anhui University of Technology, Ma'anshan, 243002, P. R. China

[c] Anhui Province Key Laboratory of Efficient Conversion and Solid-State Storage of Hydrogen & Electricity, Anhui University of Technology, Maanshan, Anhui 243002, China

[d] School of Materials Science and Engineering, Anhui University of Technology, Ma'anshan, 243002, P. R. China

[e] School of Microelectronics and Data Science, Anhui University of Technology, Ma'anshan, 243002, P. R. China

[f] SVOLT Energy Technology Co., Ltd, Changzhou, 213299, P. R. China

[*] Corresponding Authors: Haijin Li, lihaijin@ahut.edu.cn; Yongtao Li, liyongtao@ahut.edu.cn; Xiaofang Liu, xfliu2003@163.com.

Experimental section

1. Chemicals and regents

Zinc nitrate hexahydrate ($Zn(NO_3)_2·6H_2O$), Cobalt chloride hexahydrate ($CoCl_2·6H_2O$) was purchased from Sinopharm Group Chemical Reagent Co. Iron chloride hexahydrate ($FeCl_3·6H_2O$) and Nickel chloride hexahydrate ($NiCl_2·6H_2O$) were purchased from Aladdin. All of the used regents were not purified.

2. The preparation of catalysts.

In a typical synthesis strategy, 0.5 mmol $FeCl_3·6H_2O$, 0.5 mmol $NiCl_2·6H_2O$, 0.5 mmol $CoCl_2·6H_2O$ and 10 mmol $Zn(NO_3)_2·6H_2O$ were dissolved in a 50 mL methanol (donated as solution A). 5 g of 2-methylimidazole was dissolved into 100 mL methanol (donated as solution B). Next, solution B poured into solution A and stirred vigorously at room temperature for 12 h. Centrifugal collection and dried at 80℃ for 10 h. Then the obtained precursors powder was pyrolyzed at 800, 900, 1000, 1100℃, which donated as FeCoNi/NC pyrolyzed at T (T=800, 900, 1000, 1100℃).

3. Physical Characterization

The crystal structure of catalysts was analyzed by Powder X-ray diffraction

(MiniFlex-600, Rigaku, Japan). The field emission scanning electron microscope (FESEM, FEI, NANO SEM430, 15 kV) was applied to analyses the morphology of samples. The transmission electron microscope (TEM, JEM-2100, Japan) was applied to further observe the morphology of catalysts. The chemical states of elements on the surface of prepared catalysts were analyzed by X-ray photoelectron spectrometer (XPS, Thermo Scientific ESCALAB Xi+, Al kα, hv = 1486.6 eV) which calibrated the binding energy with C1s (284.8 eV).

4. Electrochemical measurements

All electrochemical properties were measured on the electrochemical workstation (CHI 760E) by using a typical three electrode system which the platinum network as a counter electrode and Hg/HgO as a reference electrode. A 3 mm rotating disk electrode (RDE) and a 5 mm rotating ring disk electrode (RRDE) was used as work electrode for ORR study while catalysts loaded Ni foam (NF) was used for OER. All the measurement potentials were converted in the reversible hydrogen electrode (RHE) by the following equation:

$$E_{vs.RHE} = E^{\theta}_{Hg/HgO} + E + 0.059 \times pH \quad \text{(S1)}$$

Where E is the tested potential, and $E^{\theta}_{Hg/HgO}$ is the standard potential of Hg/HgO reference electrode.

The working electrode were prepared as follow: 5 mg of catalysts powders were dispersed in a 1 mL mixture solution (V_{Nafion} : V_{water} : $V_{ethanol}$ = 1:9:10) to form a homogeneous black ink. 8 μL of catalysts ink was pipetted to a RDE as well as 22 μL for RRDE to form the catalysts loaded at 0.57 mg cm^{-2} for ORR test. The cyclic voltametric (CV) and liner sweep voltametric (LSV) curves were tested in a 0.1 M KOH solution saturated with O_2 and Ar under various rotating speeds from 625 rpm to 2500 rpm. The electron transfer was obtained by fitting Koutecky-Levich (K–L) equation:

$$\frac{1}{J} = \frac{1}{J_K} + \frac{1}{J_d} = \frac{1}{nFkC_{O_2}} + \frac{1}{B\omega^{1/2}} \quad \text{(S2)}$$

$$B = 0.62nFAC_O D_O^{2/3} \nu^{-1/6} \quad \text{(S3)}$$

Where the J_K and J_d were presented as kinetic current density and limit diffusion

current density. n is the overall number of electron transfer number. F is Faraday constant (F=96485 C mol^{-1}). A is the area of electrode. C_O is the bulk phase concentrations of O_2 in electrolyte solution (1.2 *10^{-3} mol cm^{-3}, 0.1 mol L^{-1} KOH). N is the kinematic viscosity of the electrolyte (0.01 cm^2, 0.1 mol L^{-1} KOH). D_O is the diffusion coefficient of O_2 in the electrolyte (1.9 *10^{-5} cm^2 s^{-1}, 0.1 mol L^{-1} KOH). ω is the angular velocity of the disk (ω = 2πN, N is the linear rotation speed). When the rotating speed is expressed in rpm, the formula (S3) can be expressed (S4):

$$B = 0.2nFAC_0D_0^{2/3}\nu^{-1/6} \quad \text{(S4)}$$

The yield of hydrogen peroxide and corresponding electron transfer number was test by RRDE measurement, which calculated by the following equation:

$$H_2O_2\% = \frac{I_R/N}{I_R/N + I_D} \times 200\% \quad \text{(S5)}$$

$$n = 4 \times \frac{I_D}{I_D + I_R/N} \quad \text{(S6)}$$

where I_R and I_D were the current density of ring and disk. N is the collection efficiency (0.38) of the Pt ring of RRDE.

5. Home-made Zn-air battery prepared and measurement

The performance of catalysts in the realm of Zn-air batteries (ZABs) was examined using a homemade ZABs system. The experimental setup involved utilizing a 3 mm thick zinc plate as the metal anode, while a catalyst-loaded carbon paper served as the air cathode. The electrolyte solution consisted of 6.0 mol L^{-1} KOH containing 0.20 mol L^{-1} Zinc acetate. To assess the battery's charge and discharge cycling capabilities, as well as its rate of performance, measurements were taken using a Neware test system.

Figures

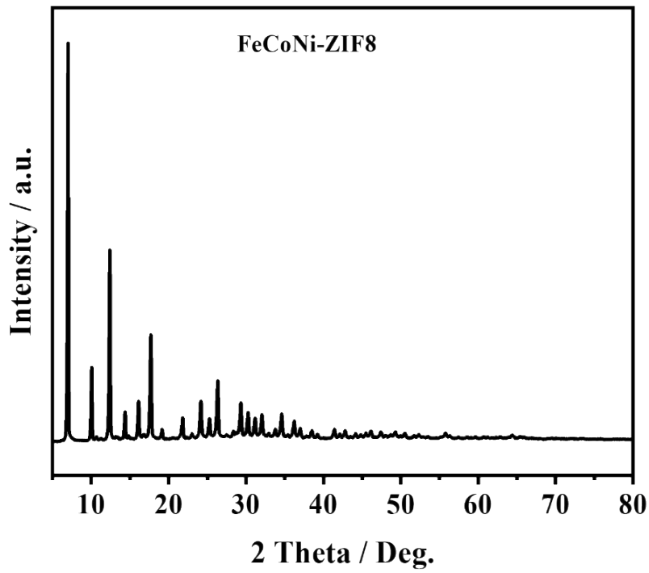

FigureS1 XRD pattern of FeCoNi-ZIF8 precursors.

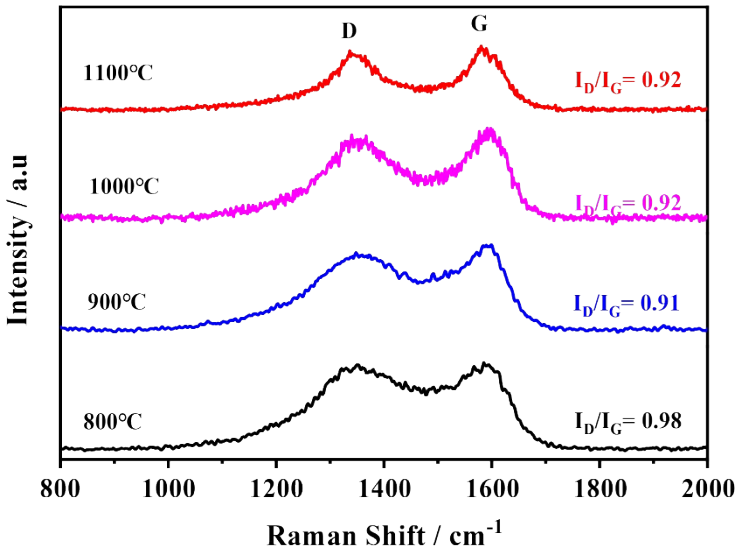

FigureS2 Raman pattern of FeCoNi/NC pyrolyzed at 800, 900, 1000 and 1100℃

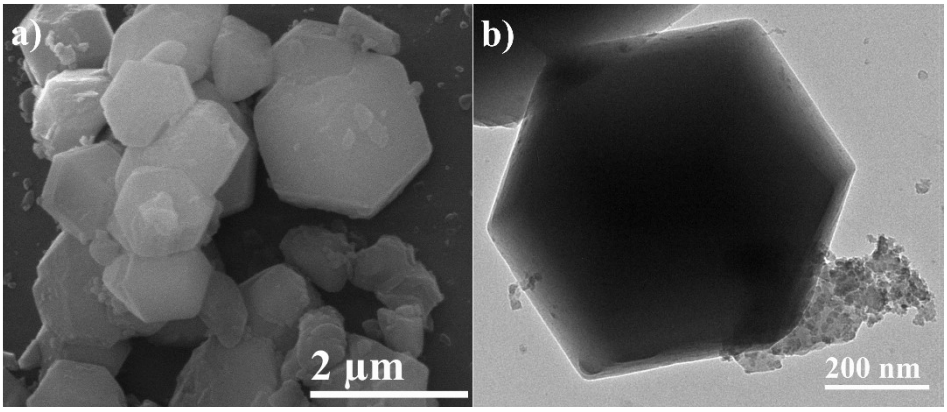

FigureS3 (a) SEM images and (b) TEM images of FeCoNi-ZIF8 precursors.

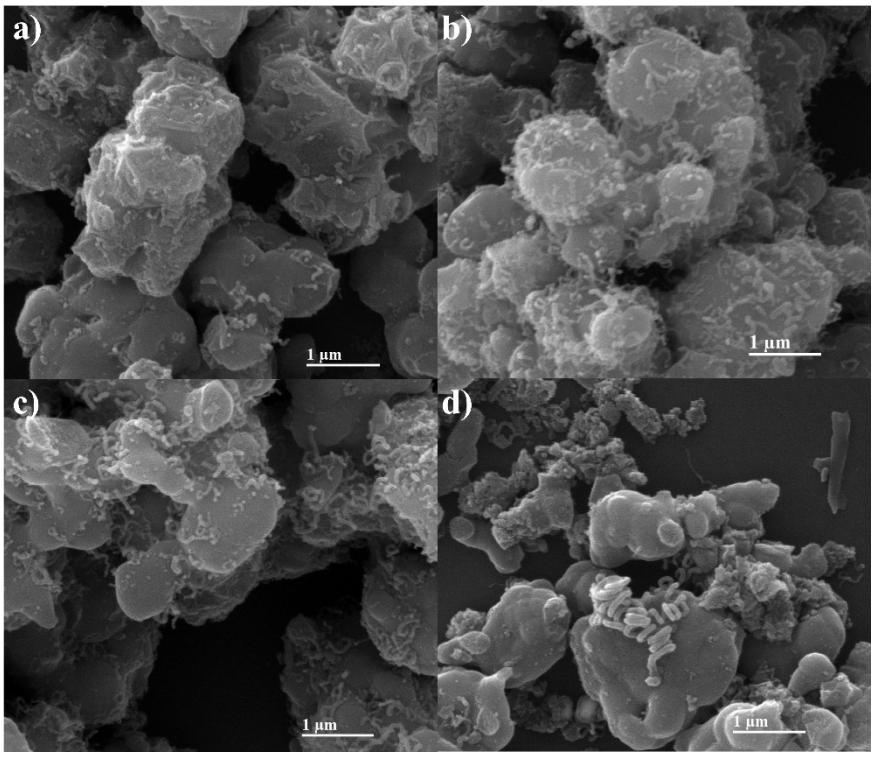

Figure S4 SEM images of (a)FeCoNi/NC pyrolyzed at 800℃, (b) FeCoNi/NC pyrolyzed at 900℃, (c) FeCoNi/NC pyrolyzed at 1000℃, (d) FeCoNi/NC pyrolyzed at 1100℃, respectively.

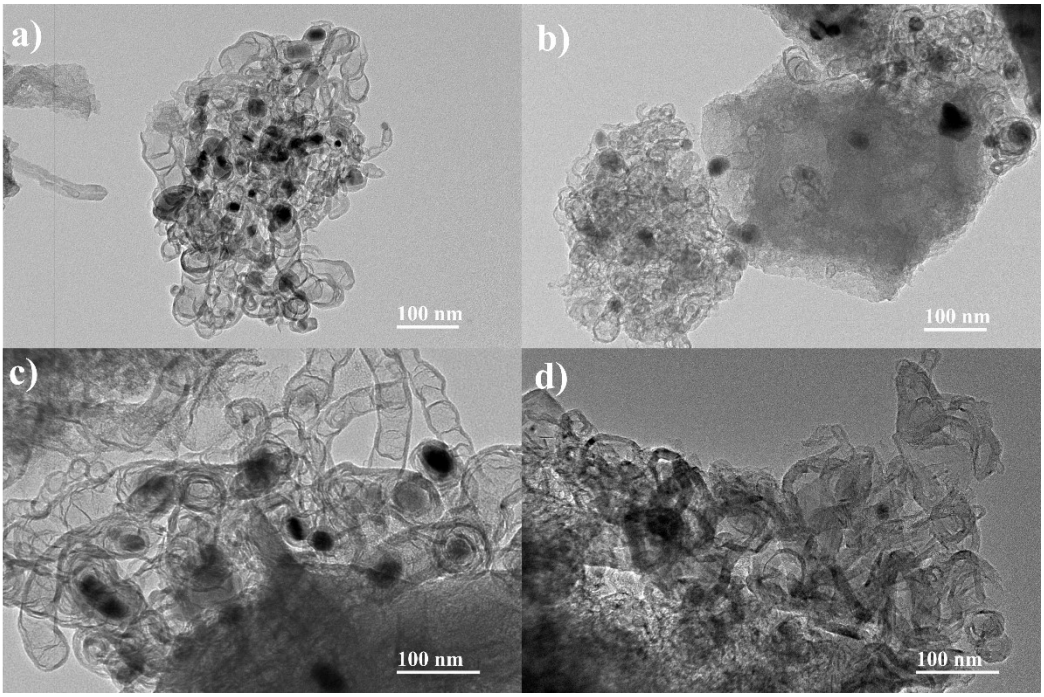

Figure S5 TEM images of (a)FeCoNi/NC pyrolyzed at 800℃, (b) FeCoNi/NC pyrolyzed at 900℃, (c) FeCoNi/NC pyrolyzed at 1000℃, (d) FeCoNi/NC pyrolyzed at 1100℃, respectively.

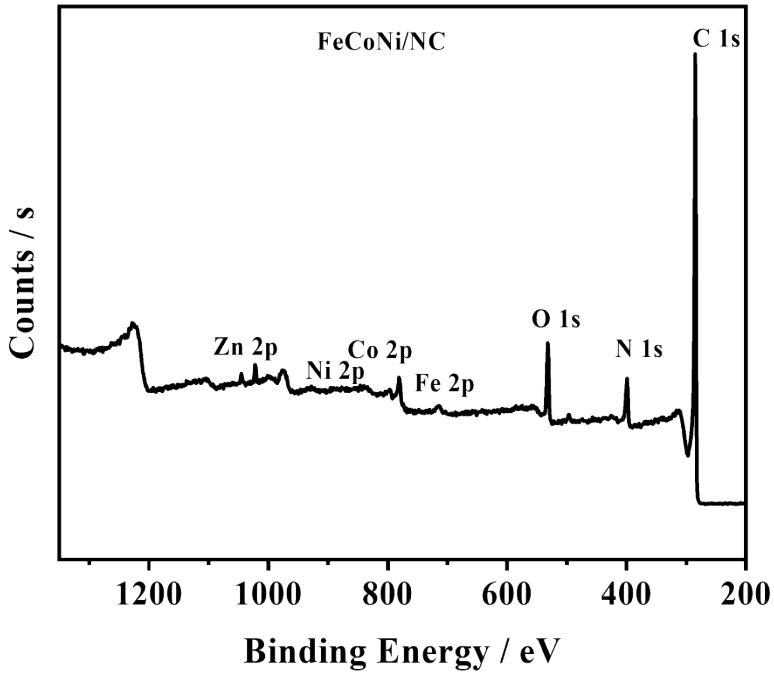

Figure S6 The survey spectrum of FeCoNi/NC pyrolyzed at 900℃.

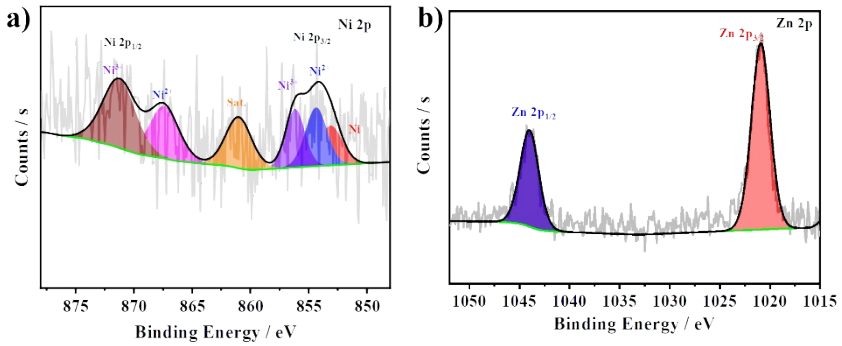

Figure S7 The high-resolution spectra of Ni 2p (a) and Zn 2p (b) of FeCoNi/NC pyrolyzed at 900℃.

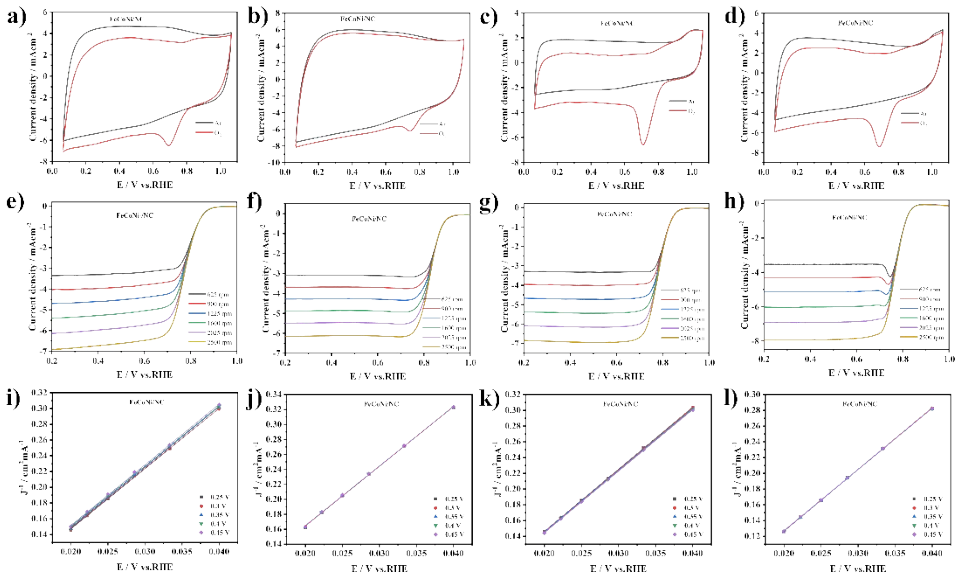

Figure S8 (a-d) CV curves of FeCoNi/NC pyrolyzed at 800, 900, 1000, 1100℃. (e-h) LSV curves at various rotating of FeCoNi/NC pyrolyzed at 800, 900, 1000, 1100℃. (i-l) K-L plot curves of FeCoNi/NC pyrolyzed at 800, 900, 1000, 1100℃, respectively.

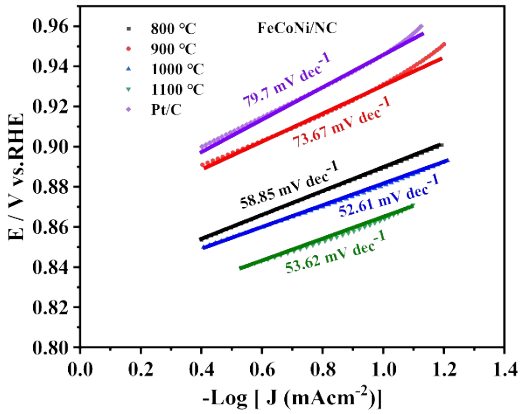

Figure S9 Tafel plot curve of FeCoNi/NC pyrolyzed at 800, 900, 1000, 1100℃ and Pt/C.

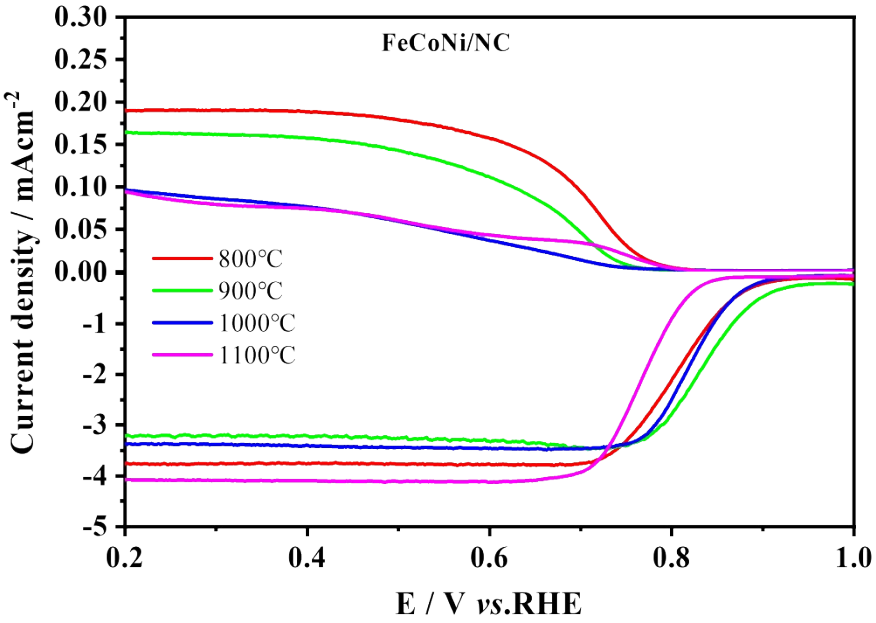

Figure S10 Polarization curves of FeCoNi/NC pyrolyzed at 800, 900, 1000 and 1100℃ measured by RRDE test.

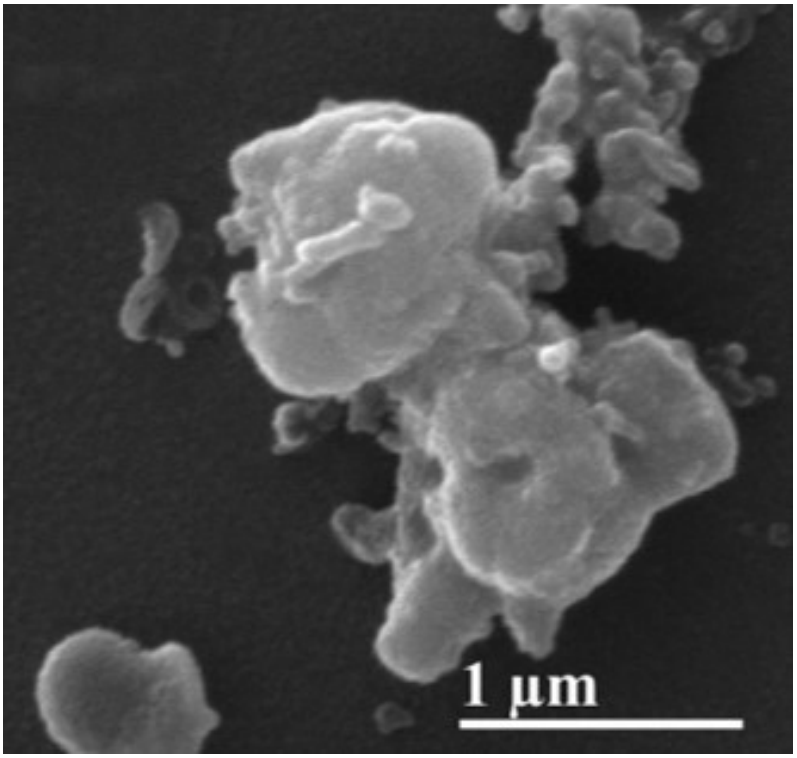

Figure S11 SEM images of FeCoNi/NC pyrolyzed at 900℃ after 50,000 i-t tests.

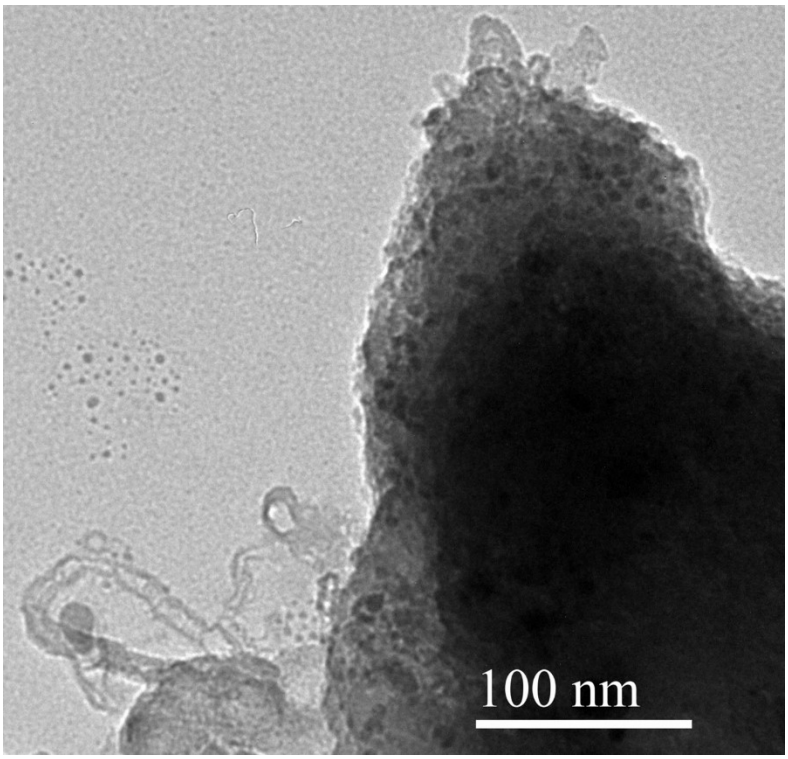

Figure S12 SEM images of FeCoNi/NC pyrolyzed at 900℃ after 50,000 i-t test

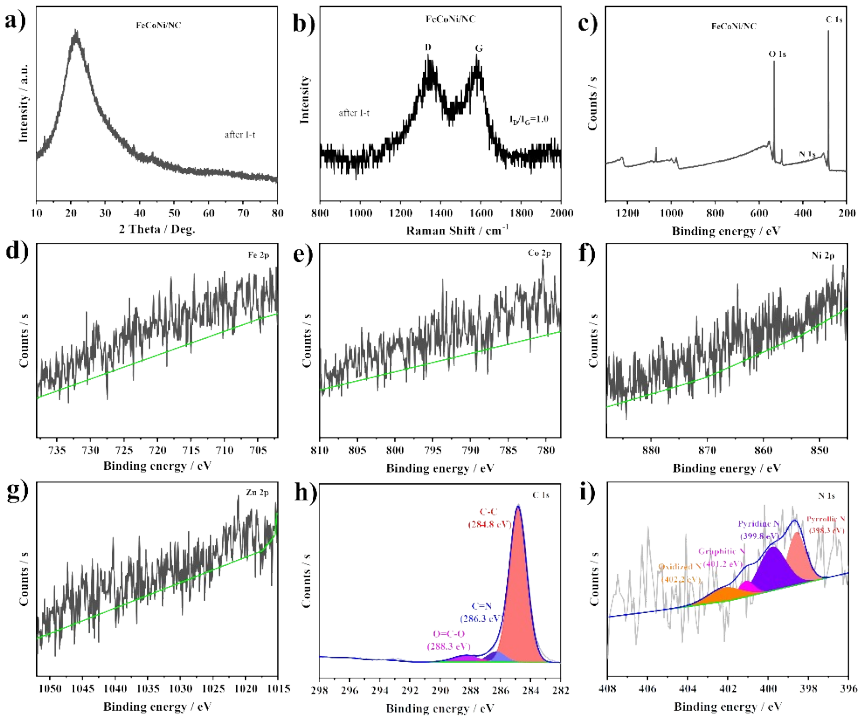

Figure S13 (a) XRD pattern, (b) Raman spectra, (c) survey spectra, (d) Fe 2p spectra, (e) Co 2p spectra, (f) Ni 2p spectra, (g) Zn 2p spectra, (h) C 1s spectra, (i) N 1s spectra of FeCoNi/NC pyrolyzed at 900℃ after I-t test.

Table S1 the element contents characterized by the EDS mapping of FeCoNi/NC pyrolyzed at 900℃

Element	Atomic % / wt.%
C	78.207
N	18.763
Fe	0.064
Co	2.284
Ni	0.135

Table S2 the element contents characterized by ICP-OES of FeCoNi/NC pyrolyzed at 900℃

Element	Element content / %
Fe	0.207
Co	5.111
Ni	0.107

Table S3 the onset potential and half-wave potential of the prepared catalysts.

Sample	Onset potential (V vs. RHE)	Half-wave potential (V vs. RHE)
FeCoNi/NC 800℃	0.94	0.82
FeCoNi/NC 900℃	0.96	0.85
FeCoNi/NC 1000℃	0.94	0.81
FeCoNi/NC 1100℃	0.88	0.79
Pt/C	0.98	0.84

Table S4 ORR and ZAB performance comparison tables reported in some previous paper.

Catalysts	ORR		ZABs			Ref
	$E_{1/2}$	electrolyte	V_{OCP}	Power density	electrolyte	
FeCoNi/NC	0.84 V (vs. RHE)	0.1 M KOH	1.5 V	161 mW cm^{-2}	6M KOH + 0.2 M $Zn(ac)_2$	This work
FeCoNi-N/CNFs	0.61 V (vs Ag/AgCl)	0.5 M H_2SO_4	——	——	——	1
FeCo/FeCoNi@NCNTs -HF	0.85 V (vs. RHE)	0.1 M KOH	1.481 V	156.22 mW cm^{-2}	6M KOH +0.2 M $Zn(ac)_2$	2
FeCoNi-N-rGO	0.836 V (vs. RHE)	0.1 M KOH	1.43 V	152.5 mW cm^{-2}	6M KOH + 0.2 M $Zn(ac)_2$	3
NiFeCo-NC2	0.620 V (vs. RHE)	0.1 M KOH	1.44 V	——	6 M KOH + 4 % ZnO electrolyte (2 mL)	4
FeCoNi-CNTs-2	0.82 V (vs. RHE)	1 M KOH	1.49 V	210.5 mW cm^{-2}	6M KOH + 0.2 M $Zn(ac)_2$	5
FeCoNi/NC	0.83 V (vs. RHE)	0.1 M KOH	1.372 V	125 mW cm^{-2}	gel electrolyte	6
FeCoNi/NCHNs	0.885 V (vs. RHE)	0.1 M KOH	1.48 V	160 mW cm^{-2}	6M KOH + 0.2 M $Zn(ac)_2$	7
Co-FeNi-342	0.86 V (vs. RHE)	0.1 M KOH	1.32 V	77 mW cm^{-2}	6M KOH + 0.2 M $Zn(ac)_2$	8
SPAN-FCNM	0.71 V (vs. RHE)	0.1 M KOH	——	242 mW cm^{-2}	6M KOH + 0.2 M $Zn(ac)_2$	9
NiFe-MOF/$NiFe_2O_4$	——	0.1 M KOH	1.397 V	158.4 mW cm^{-2}	6M KOH + 0.2 M $Zn(ac)_2$	10
$Fe_{1.2}(CoNi)_{1.8}S_6$	0.81 V (vs. RHE)	0.1 M KOH	1.45 V	158.4 mW cm^{-2}	6M KOH + 0.2 M $ZnCl_2$	11
CoFeNi/NC	0.842 (vs.RHE)	0.1 M KOH	——	——	——	12
Commercial Pt/C	0.84 (vs.RHE)	0.1 M KOH	1.38 V	146 mW cm^{-2}	6M KOH + 0.2 M $ZnCl_2$	This work

Reference

1. Q. Liu, S. Cao, Y. Fu, Y. Guo and Y. Qiu, *J. Electro. Chem*., 2018, **813**, 52-57.
2. Z. Wang, J. Ang, B. Zhang, Y. Zhang, X. Y. D. Ma, T. Yan, J. Liu, B. Che, Y. Huang and X. Lu, *Appl. Catal. B: Environ*., 2019, **254**, 26-36.
3. X. Chen, D. Chen, G. Li, C. Gong, Y. Chen, Q. Zhang, J. Sui, H. Dong, J. Yu, L. Yu and L. Dong, J. Alloy. Compd., 2021, **873**, 159833.
4. M. Etesami, R. Khezri, A. Abbasi, M. T. Nguyen, T. Yonezawa, S. Kheawhom and A. Somwangthanaroj, *J. Alloy. Compd*., 2022, **922**, 166287.
5. H. Fang, H. Bian, B. Hu, J. Liu, S. Li, M. Wang, L. He and Z. Zhang, *Appl. Surf. S*ci. 2022, **604**, 154590.
6. Q. Jin, L. Xiao, W. He, H. Cui and C. Wang, *Green Energy Environ.*, 2022, DOI: 10.1016/j.gee.2022.03.008.
7. Y. Chen, X. Meng, C. Fan, G. Yu, X. Wang, Q. Zhang, B. Pang, L. Yu and L. Dong, *Diamond Rel. Mater*., 2023, **137**, 110095.
8. C. Han, W. Li, W. Li, L. Yang and Z. Huang, *Inorganic Chem. Commu*n., 2023, **149**, 110402.
9. C.-L. Huang, Z.-F. He, J.-Y. Pai, Y.-H. Yang, W.-Y. Jao, C.-Y. Lai, Y.-T. Lu, H.-Y. Ku and C.-C. Hu, *Chem. Engin. J.*, 2023, **469**, 143855.
10. T. Lan, H. Du, Y. Li, K. Qu, J. Zhao, X. Zhang, Y. Dong, Y. Zhang, X. Zhang and D. Zhang, *J. Alloy. Compd.*, 2023, **943**, 169144.
11. H. Wu, Z. Li, Z. Wang, Y. Ma, S. Huang, F. Ding, F. Li, Q. Zhai, Y. Ren, X. Zheng, Y. Yang, S. Tang, Y. Deng and X. Meng, *Appl. Catal. B Environ.*, 2023, **325**, 122356.
12. Y. Jing, Y. Cheng, L. Wang, Y. Liu, B. Yu and C. Yang, *Chem. Engin. J.*, 2020, **397**, 125539.